



1

2

3

4

5

6

7

8 **Validation of INSAT-3D sounder data with in-situ measurements and other**

9 **similar satellite observations over Indian region**

10 **M. Venkat Ratnam*, A. Hemanth Kumar, and A. Jayaraman**

11 National Atmospheric Research Laboratory, Gadanki, India

12

13 *vratnam@narl.gov.in ; Phone: +91-8585-272123; Fax: +91-8585-272018

14



15 **Abstract**

16 To date, several satellites measurements are available which can provide profiles of
17 temperature and water vapor with reasonable accuracies. However, temporal resolution remained
18 poor, particularly over topics, as most of them are polar orbiting. At this juncture, launch of
19 INSAT-3D (Indian National Satellite) by the Indian Space Research Organization (ISRO) on 26
20 July 2013 carrying multi-spectral imager covering visible to long wave infrared region made it
21 possible to obtain profiles of temperature and water vapor over Indian region with higher
22 temporal and vertical resolutions and altitude coverage besides the other parameters. The initial
23 validation of INSAT-3D data is made with the high temporal (3 h) resolution radiosonde
24 observations launched over Gadanki (13.5°N, 79.2°E) during a special campaign and routine
25 evening soundings obtained at 12 UTC. We also compared INSAT-3D data with the radiosonde
26 observations obtained from 34 India Meteorological Department stations. Comparisons were also
27 made over Indian region with data from other satellites like AIRS, MLS and SAPHIR and ERA-
28 Interim and NCEP re-analysis datasets. INSAT-3D is able to show a better coverage over Indian
29 region with high spatial and temporal resolutions as expected. Good correlation in temperature
30 between INSAT-3D and in-situ measurements is noticed except in the upper troposphere and
31 lower stratospheric region (positive bias of 2-3K). There exists mean dry bias of 10-25% in
32 relative humidity. Similar biases are also noticed when compared to other satellites and re-
33 analysis data sets. INSAT-3D shows large positive bias in temperature above 25°N in the lower
34 troposphere. Thus, caution is advised in using this data at those places for tropospheric studies.
35 Finally it is concluded that temperature data from INSAT-3D is of high quality that can be
36 directly assimilated for better forecast over Indian region.

37 **Key words:** Temperature, relative humidity, INSAT-3D, radiosonde, MLS, AIRS, reanalysis.



38 **1. Introduction**

39 Temperature and water vapor play an important role in deciding the thermodynamic state
40 of the atmosphere as they are considered as feedback parameters which alter the radiation and
41 moist dynamics of the atmosphere. The stability of the Earth's atmosphere (troposphere and
42 stratosphere) depends on the density of the air parcel at any particular altitude. The density of the
43 air parcel depends on the amount of water vapor present in it and also its temperature. The water
44 vapor is a highly varying parameter which is mainly responsible for precipitation and all other
45 weather systems. It is the source of the latent heat which is released into the atmosphere during
46 the cloud formation. It also dominates the structure of diabatic heating of the Earth's atmosphere
47 (Trenberth et al., 2005; Trenberth and Stepaniak, 2003a; 2003b). These parameters vary in time
48 and as well as in space (both vertically and horizontally) throughout the atmosphere.

49 Profiles of temperature (T) and relative humidity (RH) water vapor are traditionally
50 obtained from the in-situ conventional radiosonde measurements which have high vertical
51 resolutions and accuracies. However, they have limited spatial and temporal coverage. For this
52 reason, the satellites are considered as the best source of information for obtaining these
53 parameters which provide observations on a global scale and with improved temporal resolution
54 based on the orbit in which the satellite is present. Among several satellites, Atmospheric
55 Infrared Sounder (AIRS), Microwave Limb Sounder (MLS) and GPS Radio Occultation provide
56 profiles of temperature and water vapor with reasonable accuracies. Recently Sounder for
57 Atmospheric Profiling of Humidity in the Inter-tropical Regions (SAPHIR) onboard Megha
58 Tropiques has been introduced which provides profiles of RH in the tropical latitudes (Venkat
59 Ratnam et al., 2013). They have good spatial coverage but the temporal resolution of these
60 satellites is poor. At this juncture launch of Indian National Satellite System (INSAT)-3D in July



61 2013 has gained lot of significance due to its geostationary transfer orbit which provides profiles
62 of T and RH with high temporal resolutions, though restricted to Indian region only when
63 compared to other satellites mentioned above. This data is expected to play important role in
64 numerical weather prediction over Indian region. Before using this data for weather forecasting,
65 it is essential to validate with in-situ, similar satellite and re-analysis data sets.

66 In this report, we discussed the features of T and RH obtained from INSAT-3D sounder.
67 It adds a new dimension by providing continuous observations of T and RH over the Indian
68 region and thereby useful in monitoring the Earth's weather systems continuously. In the first
69 section we compared the broad features of T and RH obtained from INSAT-3D with the other
70 satellite observations. It is followed by the validation of INSAT-3D data with high resolution
71 radiosonde launched during a special campaign (Tropical Tropopause Dynamics Campaigns)
72 (Venkat Ratnam et al., 2014) and routine evening soundings over Gadanki (13.5°N, 79.2°E), a
73 tropical station in the southern peninsular India. We also compared this data with the India
74 Meteorological Department (IMD) network of radiosonde consisting of 34 stations over Indian
75 region. In this context it is worth to quote Mitra et al. (2015) where they compared INSAT-3D
76 data obtained from January 2014 to May 2014 with 10 GPS stations of IMD. However, their
77 work is restricted up to 100 hPa only and for initial 5 months. In the present work we extended
78 comparisons for complete 2 years (2014 and 2015) and up to 10 hPa. Further, the comparisons
79 are also made with other satellite observations like AIRS (Atmospheric Infrared Sounder),
80 Microwave Limb Sounder (MLS), and SAPHIR (Sounder for Atmospheric Profiling of Humidity
81 in the Inter-tropical Regions) and re-analysis data sets like ERA-Interim (European Center for
82 Medium Range Weather Forecasts ECMWF), NCEP (National Center for Environmental
83 Prediction).



84 **2. Database**

85 **2.1. INSAT-3D**

86 The INSAT-3D which is considered to be the advanced version of all the other INSAT
87 series satellites is the meteorological satellite of ISRO launched from Kourou, French Guiana as
88 a passenger payload along with AlphaSat / InmarSatI-XL, ESA/ InmarSat by the European
89 launch vehicle named Ariane-5 VA-214 on 26 July 2013. It was positioned at 82°E over the
90 equator at an altitude of 35,786 km from the surface of Earth in the Geostationary Transfer Orbit
91 (GTO) with the main objectives of monitoring the earth and ocean continuously thereby
92 providing the data dissemination capabilities. It also provides an operational, environmental and
93 storm warning system to protect the life and property. It carries four payloads namely the multi-
94 spectral imager (optical radiometer) which provides the high resolution images of the mesoscale
95 phenomena and local storms mainly in the visible band, apart from imaging the whole earth disk
96 in the shortwave Infrared, middle Infrared, water vapor and low thermal Infrared channels. The
97 atmospheric sounder which has 19 channels in shortwave infrared, middle infrared, long wave
98 infrared (18) and visible (1) channel measures the irradiance and provides the profiles of T, RH
99 and integrated ozone over the selected land mass of the Indian region every hour and whole
100 Indian ocean every six hours as show in Table 1.

101 This atmospheric sounder gives profiles of T and RH at 40 pressure levels (1000, 950,
102 920, 850, 750, 700, 670, 620, 570, 500, 475, 430, 400, 350, 300, 250, 200, 150, 135, 115, 100,
103 85,70,60, 50, 30, 25, 20, 15, 10, 7, 5, 4, 3, 2, 1.5, 1, 0.5,0.2, 0.1 hPa) for every one hour at 10 km
104 x 10 km in latitude and longitude resolutions covering 5-40°N and 60-100°E over India region.
105 The INSAT-3D sounder provides T and RH profiles along with the total columnar ozone from
106 the Infrared radiances obtained in different absorption bands during the clear sky conditions. The



107 retrieval algorithm adopted for INSAT-3D sounder is same as that adopted for HIRS (High
108 resolution Infrared radiation sounder) and GOES sounder which are mainly based on the
109 retrieval algorithm of Hayden (1988), Ma et al. (1999) and Li et al. (2000).

110 **2.2. Radiosonde observations**

111 The processed and quality checked radiosonde data obtained from the Integrated Global
112 Radiosonde Archive (Durre et al., 2006) over Indian region at different locations (0-40° N, 60-
113 100° E) during the period 2014-2015 are obtained. The observed unexpected sharp spikes in the
114 data are removed and the data values which are within the range $\pm 2\sigma$ are only considered for
115 comparison. Such stringent quality checked data obtained are utilized for comparing with the T
116 and RH obtained from INSAT-3D. The 34 locations of the radiosonde stations over the Indian
117 region (i.e., IMD stations) are shown in the Figure 1. The data from these IMD stations obtained
118 at 00 UTC are only used for comparison as the 12 UTC data during this period is very sparse.

119 Further, high altitude resolution GPS radiosondes (Meisei RS-11 G, Japan) that were
120 launched over Gadanki around 12 UTC are also used in the present study. Besides these routine
121 evening radiosonde launches, the radiosondes that were launched as a part of special campaign
122 between January 2014 and March 2014 over the same location are also utilized for comparison at
123 sub-daily scales. The sensors used for measuring the T and RH are thermistors and carbon
124 hygristors, respectively. The range of the T and RH measured by the sensors are -90 to +50 ° C
125 and 1-100 % with an accuracy of 0.5 K and 5-7 %, respectively (Basha and Ratnam, 2009;
126 Venkat Ratnam et al., 2014). During this campaign the radiosondes were launched for every 3
127 hours (11:30, 14:30, 17:30, 20:30, 23:30, 02:30, 05:30 and 08:30 IST) continuously for three
128 consecutive days. The entire radiosonde datasets are interpolated to the pressure levels of
129 INSAT-3D data.



130 **2.3. Other satellite observations**

131 **2.3.1. AIRS observations**

132 AIRS is one of the payloads on the NASA Earth Observing System satellite called
133 AQUA which is in a polar sun synchronous orbit revolving at an altitude of 705 km from the
134 Earth's surface with an orbital period 98.99 minutes. It completes approximately 14.5 orbits per
135 day and the separation between any two consecutive orbits near the equator is 2760 km. The
136 partner payloads along with AIRS onboard AQUA satellite are microwave instruments AMSU
137 and Humidity Sounder for Brazil. The satellite crosses the equator twice a day one being during
138 the ascending node at ~13:30 UTC and the other one being during the descending node at ~01:30
139 UTC. It is a high spectral sounder with 2378 channels measuring the IR radiances at wavelengths
140 in the range of 3.7–15.4 μm with a swath of 1,650 km and horizontal spatial resolution of 13.5
141 km at nadir (Aumann et al., 2003). We used the level 3 version 5 daily gridded data products
142 (Susskind et al., 2006) that are obtained from the IR radiances of AIRS sounder during 2014 and
143 2015. The level 3 data products (AIRS V5 L3) are obtained from the level 2 swath data where
144 the data of all the 15 orbits of the day are averaged together and the data has a latitudinal and
145 longitudinal resolution of $1^\circ \times 1^\circ$ at 24 pressure levels for T starting from 1000hPa to 1hPa and 12
146 levels for RH from 1000hPa to 100hPa. Note that RH data is reliable in the first 8 levels from the
147 surface and up to 300 hPa (Waters et al., 2006).

148 **2.3.2. MLS observations**

149 MLS is one of the four payloads onboard NASA's EOS Aura satellite which is one
150 among the six satellites (OCO-2, GCOM-W1, AQUA, CLOUDSAT, CALIPSO, AURA) that
151 form the A-Train constellation. Similar to AIRS, MLS is also a polar orbiting sun synchronous
152 satellite (AURA) which is at ~705 km, scanning its view from ground to ~90 km at 55 pressure



153 levels with a global view covering from 82° S to 82° N by having ~15 orbits per day. It scans the
154 Earth's atmosphere for every 25 seconds and provides 240 scans per orbit. The details regarding
155 the MLS measurement technique, instrumentation are discussed by Waters et al. (2006). The
156 MLS measures the thermal emission of the earth through its limb viewing geometry at
157 microwave band centered near 118 GHz, 190 GHz, 240 GHz, 640 GHz and 2500 GHz whose
158 retrieval algorithm can be found from Livesey et al. (2006). We made use of the Level 2 version
159 3 temperature and water vapor data during the period 2014 and 2015 that was downloaded from
160 <http://mirador.gsfc.nasa.gov>. Note that water vapor from this instruments is more valid above
161 300 hPa only (Basha et al., 2013).

162 **2.3.3. SAPHIR observations**

163 SAPHIR is one of the four instruments onboard Megha Tropiques (MT) satellite which is
164 moving in a circular low inclination orbit at 20° with 14 orbits per day. It provides a cross track
165 scan of ±43° with a swath of 1705 km and resolution of 10 km at nadir. It is a passive remote
166 sensing microwave sounder which operates at 6 channels close to 183.31 GHz (±11.0, ±6.60,
167 ±4.30, ±2.8, ±1.2) retrieving integrated RH of the entire troposphere from brightness temperature
168 at 1000-850 hPa, 850-700 hPa, 700-550 hPa, 550-400 hPa, 400-250 hPa and 250-100 hPa within
169 ±30° latitudinal belt. The algorithms related to retrieval for the sounders of MT satellite are
170 discussed by Gohil et al. (2012). This data has been validated against similar satellites and
171 reanalysis data sets and found good except in level 1 (1000-850 hPa) (Venkat Ratnam et al.,
172 2013). We made use of the SAPHIR data for comparison which was downloaded from
173 www.mosdac.gov.in for the period 2014 and 2015.

174

175



176 **2.4. Re-analysis datasets**

177 **2.4.1. ERA-Interim data**

178 ERA-Interim is the advanced global atmospheric reanalysis which is produced by
179 ECMWF. It provides gridded data products which include large surface parameters for every 3
180 hours and upper air parameters covering troposphere and stratosphere for every 6 hours starting
181 from 1979 onwards. The data products are obtained from the model through sequential data
182 assimilation method where the models are fed with the available observations to forecast the
183 evolving state of the global atmosphere. The configuration and performance of the ERA-Interim
184 reanalysis is explained clearly by Dee et al. (2011). It is even considered as the latest and most
185 advanced global assimilation scheme which can predict the atmosphere at the nearest accuracy to
186 what is theoretically possible (Simmons and Hollingsworth, 2002; Simmons et al., 2007). These
187 data products are available over the entire globe at different latitude and longitude resolutions
188 and for 37 pressure levels from 1000 hPa to 1 hPa. We have made use of $1^\circ \times 1^\circ$ data products of T
189 and RH for the period 2014 and 2015.

190 **2.4.2. NCEP/NCAR data**

191 This data set is a joint product of National Centers for Environmental Prediction (NCEP)
192 and National Center for Atmospheric Research (NCAR). Similar to ERA-Interim data this is also
193 provides gridded data which is available from 1948 onwards. NCEP data represents the state of
194 Earth's atmosphere by incorporating the global historical observations and the output of global
195 numerical weather prediction (NWP) model (Kalnay et al., 1996). These data products are
196 available all over the globe at $2.5^\circ \times 2.5^\circ$ latitude –longitude resolution at 17 pressure levels
197 starting from 1000 hPa to 10 hPa for temperature and 8 pressure levels for RH from 1000 hPa to
198 300 hPa. We made use of this data for T and RH during the period of 2014 and 2015.



199 **3. Results and discussion**

200 **3.1. Spatial variation of T and RH over Indian region**

201 In this section, the observations of the advanced ISRO geostationary INSAT-3D satellite
202 sounder which provides continuous observations over land and ocean of Indian region are
203 discussed as they are very important in weather forecasting. The continuous observations of the
204 sounder are very much important as these observations can be introduced and combined with
205 model output for a better forecast of the Earth's atmosphere. Before it is used for any scientific
206 purpose, it is essential to compare / validate with other similar data sets. Figure 1 shows the
207 spatial variation of T and RH over Indian region at 850 hPa pressure level obtained from INSAT-
208 3D satellite on 2 May 2015 (averaged over a day). White patches show the non-availability of
209 the data due to topography (Himalayan Mountains). Higher temperatures of about 5-6 K over the
210 main land mass than surrounding sea can be noticed. On the contrary, very low values of RH
211 over the land mass than surrounding ocean can be noticed.

212 The simultaneous observations from MLS and AIRS over the Indian region obtained
213 around 13:30 IST (i.e., ascending node for AIRS and MLS) on the same day is considered for
214 comparison. Spatial variation of T and RH over Indian region observed at 500 hPa pressure level
215 from INSAT-3D, MLS and AIRS satellites on 2 May 2015 around 13:30 IST is shown in Figure
216 2. Spatial variation of T and RH over Indian region obtained from ERA-Interim and NCEP at the
217 same pressure level at 06 UTC (11:30 IST) is also shown. In general, though major features in
218 the spatial variation of T resembles among different satellites and re-analysis data sets, however,
219 large difference in the RH is noticed. Particularly AIRS show large RH variations over Bay of
220 Bengal (BoB) and Himalayan region when compared to other two satellites. Similar high
221 variation in RH is also seen by ERA-Interim (Figure 2i). Very low RH values in the central India



222 and toward west in all the satellite observations can be noticed. The quantitative difference
223 between INSAT-3D and other satellite measurements and re-analysis data sets will be discussed
224 in later sections.

225 **3.2. Comparison between INSAT-3D and radiosonde observations at sub-daily scales**

226 INSAT-3D sounder provides the profiles of T and RH over Indian region for almost
227 every hour. It is desirable to compare these profiles at different timings of the day which is
228 difficult to do with existing polar satellites. Thus, we compared the INSAT-3D profiles of T and
229 RH with radiosonde observations obtained over Gadanki and also using IMD network of
230 radiosondes. It is well known that the most common and widespread in-situ instruments for
231 providing accurate profiles of T and RH are radiosondes. However, accurate measurements of
232 RH are found to be a challenging task with the help of radiosondes in the upper troposphere and
233 lower stratosphere where the concentration of water vapor is very low. In addition to this there
234 exists radiation error in temperature measurements as explained by Luers and Eskridge, (1998)
235 and Wang et al. (2003). We have used high accuracy and vertical resolution radiosonde over
236 Gadanki that were launched for every 3 hours continuously for three consecutive days, during a
237 special campaign called Tropical Tropopause Dynamics campaign (TTD) (Venkat Ratnam et al.,
238 2014) conducted over Gadanki between January 2014 and March 2014. This data is used to
239 validate the INSAT-3D measurements at sub-daily scales.

240 The radiosonde data obtained during the TTD campaigns are interpolated to the pressure
241 levels of INSAT-3D for the similar hours whenever observations are available. Typical temporal
242 variation of T and RH obtained from radiosonde launched over Gadanki during one of the TTD
243 campaigns conducted from 27 January 2014 to 30 January 2014 is shown in Figure 3. Data
244 obtained from INSAT-3D for similar timings are also shown in the bottom panels. White patches



245 show the non-availability of the data. In general, similar diurnal variation in the T and RH
246 between radiosonde and INSAT-3D can be noticed though the magnitude differs. Very cold
247 temperatures (~190 K) present near the tropopause region (100 hPa) are captured well by
248 INSAT-3D. The existence of high humidity layer at 300 hPa, persisting for more than a day, is
249 also captured well by the INSAT-3D. The T and RH over Gadanki obtained from INSAT-3D and
250 radiosonde are averaged over 3 days and the mean and standard deviation are shown in Figure
251 3(e) and 3(f), respectively. From these profiles, no significant difference in the T can be noticed
252 but there exists underestimation in RH by INSAT-3D (assuming radiosonde as standard
253 technique). INSAT-3D shows a dry bias of 20-35% in RH when compared to radiosonde
254 observations. No significant day-night differences are noticed between INSAT-3D and
255 radiosonde observations.

256 **3.2. Comparison between INSAT-3D and radiosonde (IMD and Gadanki) observations**

257 We also compared INSAT-3D measurements obtained during 2014 and 2015 with the
258 radiosonde observations over the 34 IMD stations which are spread throughout the Indian region
259 whose locations are shown in the form of filled circles in Figure 1. Besides these, the routine
260 evening radiosonde observations launched around 12 UTC over Gadanki during 2014 and 2015
261 were also utilized for day-to-day comparisons. The radiosonde data of all the IMD stations are
262 interpolated to the pressure levels of INSAT-3D for uniformity. The correlation co-efficient
263 values obtained for T and RH between INSAT-3D and Gadanki radiosonde launched around 12
264 UTC and IMD radiosonde launched around 00 UTC over Indian region are obtained separately
265 for each day during the period 2014 and 2015. The correlation values are obtained for all the
266 levels in T whereas only up to 300 hPa in RH and is shown in Figure 4. A very high correlation
267 (>0.8) in T between INSAT-3D and IMD /Gadanki radiosonde is observed in the lower



268 troposphere (Figure 4a). However, correlation decreases above 700 hPa (850 hPa) between
269 INSAT-3D and Gadanki (IMD) radiosonde. There exists consistent correlation of more than 0.6
270 throughout all levels with Gadanki radiosonde but drastically decreases above 250 hPa in case of
271 IMD radiosondes. It is interesting to notice higher (lower) correlation below (above) 850 hPa
272 between Gadanki radiosonde and INSAT-3D. However, it is quite opposite in case of IMD
273 radiosonde for which reasons are not known. The correlation values of RH obtained between
274 INSAT-3D and Gadanki radiosonde is always higher (greater than 0.65) throughout the profile
275 than the correlation obtained between INSAT-3D and IMD radiosonde observations (less than
276 0.5) shown Figure 4b. Mitra et al. (2015) has reported similar correlations using 10 IMD stations
277 using 5 months (January 2014- May 2014) of the data. However, their work is restricted up to
278 100 hPa due to frequent balloon burst of IMD radiosondes at that altitude. In the present study
279 we report up to 10 hPa and also using complete two years of the data for Gadanki location. The
280 observed good correlation (0.6-0.7) between INSAT-3D RH and Gadanki radiosonde RH may be
281 attributed to the improved RH sensor used in Meisei radiosondes that were used over Gadanki.

282 Further, to quantify the differences between INSAT-3D and Gadanki radiosonde, we
283 discuss the fractional difference at all levels between routine radiosondes launched around 12
284 UTC over Gadanki and INSAT-3D T over the same site during the period 2014 and 2015. The
285 fractional difference of T for each day is calculated separately and then averaged over 2014 and
286 2015. The balloon bursting altitude of the radiosonde is also estimated for those which are
287 utilized in estimating the fractional difference. The fractional difference of T and RH and balloon
288 bursting altitude are shown in Figure 5. It is clear from the figure that the difference is very less
289 in the troposphere (~ 0.5 K). The mean fractional difference in the troposphere is less than 0.5 K,
290 and it is about 1 K in the upper troposphere and lower stratosphere. However, positive bias



291 (INSAT-3D showing higher temperatures) of 2-3 K is noticed (shown as standard deviations) in
292 day-to-day differences in INSAT-3D. When we segregated season wise fractional differences,
293 higher fractional difference during monsoon season is noticed (figure not shown) mainly due to
294 less number of matches between INSAT-3D and radiosonde due to over sky. Most striking
295 feature to be noticed is the consistent positive bias of 1% (~2 K) in T in the upper troposphere
296 and lower stratosphere. The mean fractional difference in RH shown in Figure 5b reveals 20-
297 30% dry bias in INSAT-3D when compared to radiosonde. Standard deviations show dry bias of
298 40-60% in day-to-day comparison of RH between INSAT-3D and radiosonde. Thus, from figure
299 5, it is clear that INSAT-3D is able to provided T measurements with high accuracies but huge
300 dry bias is observed in RH. Thus, caution is advised while using RH data from INSAT-3D.

301 **3.2. Comparison between INSAT-3D and other satellite and re-analysis data**

302 The T and RH measured from the radiances of 19 channels of INSAT-3D sounder are
303 compared with that are obtained from other satellites like AIRS, MLS and SAPHIR (only RH)
304 during the period 2014 and 2015. Besides the satellite observations, re-analysis datasets like
305 ERA-Interim and NCEP are also utilized for comparing the data obtained from INSAT-3D. The
306 T measurements obtained from AIRS, MLS, ERA-Interim are converted to a spatial resolution of
307 $1^{\circ} \times 1^{\circ}$ in latitude and longitude. The $1^{\circ} \times 1^{\circ}$ gridded AIRS and MLS T measurements are
308 interpolated to 40 pressure levels of INSAT-3D. Whereas, the INSAT-3D data is converted to a
309 spatial resolution of $2.5^{\circ} \times 2.5^{\circ}$ to compare with the T obtained from NCEP. The difference in T
310 between INSAT-3D and AIRS and MLS are estimated for each day, whereas it is estimated for
311 every six hours between INSAT-3D and ERA-Interim and NCEP. The zonal mean latitudinal
312 difference of T between different satellites and re-analysis datasets is obtained for each day and
313 then averaged for 2014 and 2015 which is shown in Figure 6. Note that the differences that are



314 greater than 1K are only shown in this figure. In general, the difference in T between INSAT-3D
315 and other satellite and reanalysis data sets lies within ± 1 K and extends to 2 K in the UTLS
316 region. Above 25°N, INSAT-3D shows positive bias of more than 4 K up to 300 hPa compared
317 to AIRS but up to 700 hPa with rest of the data sets. Consistent positive bias of 2-3 K in the
318 UTLS region can be noticed in INSAT-3D particularly compared with other satellite
319 measurements. Above 4 hPa, consistent negative bias of more than 3 K is noticed in INSAT-3D
320 when compared to other data sets. In general, less difference between INSAT-3D and NCEP is
321 noticed than ERA-Interim. Thus, the difference in T between INSAT-3D and other datasets is
322 least in the lower and mid troposphere below 25°N, whereas it increases in the lower troposphere
323 above 25°N.

324 The RH data obtained from AIRS, MLS, ERA-Interim are converted to a spatial
325 resolution of 1° X 1° in latitude and longitude and then interpolated to the first 21 pressure levels
326 of INSAT-3D. To compare the INSAT-3D RH data with NCEP RH data, the RH data obtained
327 from INSAT-3D is converted to the actual resolution of NCEP, i.e., 2.5°X2.5° latitude and
328 longitude grids. Note that information on RH data obtained from NCEP is present only up to 300
329 hPa, MLS from 300 hPa and above, whereas RH from AIRS and ERA-Interim is considered up
330 to 100 hPa beyond which the concentration of water vapor is very low. But, the RH obtained
331 from SAPHIR in the troposphere is measured as integrated relative humidity at certain levels as
332 mentioned in the section 2. In order to compare the INSAT-3D RH data with SAPHIR RH, the
333 former is converted to the pressure levels of SAPHIR. The zonal mean latitudinal difference
334 between INSAT-3D and all other datasets is obtained as mentioned in the previous section and is
335 presented in Figure 7. In general, INSAT-3D shows a dry bias of 5-10% in the lower and mid
336 troposphere below 25°N when compared with AIRS (Figure 7a), ERA-Interim (Figure 7c) and



337 NCEP (Figure 7d) re-analysis datasets. However, it shows a dry bias of more than 10% when
338 compared with MLS RH (Figure 7b). Note that INSAT-3D also shows a wet bias around 700
339 hPa with all the datasets. A high dry bias in the lower troposphere above 25° N is observed
340 between INSAT-3D and AIRS, ERA-Interim and NCEP, whereas the bias in the same region is
341 less with MLS. The wet bias (~20%) between INSAT-3D and AIRS above 300 hPa is mainly
342 due to low accuracies of AIRS at those altitudes (Waters et al., 2006). There exists a dry bias of
343 20% between INSAT-3D and SAPHIR in first two layers but reduced to less than 10% above
344 (Figure 7e). In this context it is worth to quote findings of Venkat Ratnam et al. (2013) who have
345 reported that the first layer (1000-850 hPa) of SAPHIR has large difference when compared to
346 similar satellites. Thus, the present result of large difference between INSAT-3D and SAPHIR in
347 the lower most layers is expected. Note that no data is there in SAPHIR above 27° due to its low
348 inclination.

349 **4. Consistency check in T measurements of INSAT-3D in the UTLS region**

350 From the previous section, it is clear that INSAT-3D overestimates T by 1% in the UTLS
351 region. However, in order to check whether this positive bias is consistent or not, we compared
352 the tropopause temperature obtained from radiosonde. The cold point tropopause temperature
353 (CPT) which is the minimum in the temperature profile below 20 km is obtained from
354 radiosonde and INSAT-3D for each day during 2014 and 2015 and is shown in Figure 8.
355 Consistent positive bias of 2-3 K is seen in CPT between INSAT-3D and radiosonde as expected,
356 however, general trends match well between the two. The CPT obtained from INSAT-3D
357 matches well with the radiosonde observations and shows a clear annual variability with higher
358 values during the summer monsoon months (JJA) and lower values observed in winter months
359 (DJF). This seasonal variability of the CPT over the Indian Monsoon region during different



360 seasons is consistent with that reported by Mehta et al. (2010). These results are also consistent
361 with that reported earlier over other tropical latitudes (Newell et al., 1969; Reed and Vlcek,
362 1969; Reid and Gage, 1996; Seidel et al., 2000) who attributed it to the annual modulation of
363 Hadley cell. Thus, INSAT-3D data can be effectively utilized to investigate the tropopause
364 characteristics, however, with a known caution of overestimation of T by 2-3 K. As the data
365 from INSAT-3D is available for almost every hour this data is very much useful to investigate
366 Stratosphere Troposphere Exchange (STE) process occurring at sub-daily scales.

367 **5. Summary and Conclusions**

368 The quality of the new data product mainly the temperature and relative humidity obtained
369 from the sounder payload onboard INSAT-3D is discussed. A detailed comparison of the data
370 (temperature and relative humidity) obtained from INSAT-3D with the existing in-situ
371 radiosonde measurements over the entire Indian region, other similar satellite (AIRS, MLS and
372 SAPHIR) observations and re-analysis (ERA-Interim and NCEP) datasets has been carried out in
373 the present study. Following are the main conclusions drawn from the study.

- 374 1. INSAT-3D provides measurements with very good spatial and temporal coverage over
375 the Indian region when compared to any other satellites as expected.
- 376 2. INSAT-3D is able to measure the general features of temperature and relative humidity
377 similar to the radiosonde observations even at sub-daily scales. However, magnitudes
378 differs (underestimates) in relative humidity measured by INSAT-3D. There is no day-
379 night difference in the temperature measurements of INSAT-3D.
- 380 3. The mean difference between INSAT-3D and radiosonde temperature in the troposphere
381 is less than 0.5K with standard deviations of 1K. However, mean difference in RH is as
382 high as 20-30% with standard deviations of 40-60%.



383 4. The RH obtained from INSAT-3D shows high correlation values (0.6-0.7) with the
384 Gadanki radiosonde RH than the IMD radiosonde (less than 0.5) due to improved sensor.

385 5. There exists consistent positive bias (~ 2-3 K) in temperature in the upper troposphere
386 and lower stratosphere in INSAT-3D.

387 6. A dry bias of 10-25% in the INSAT-3D measured RH when compared to similar
388 satellites and reanalysis data sets are noticed.

389 7. In general, temperature from INSAT-3D agrees well with all the other satellite
390 measurements and reanalysis data sets below 25°N, whereas a difference of ~4K in
391 temperature above 25°N is noticed. INSAT-3D shows less temperature difference around
392 tropopause region with AIRS and ERA-Interim datasets.

393 It is found that there exists large difference between INSAT-3D and other datasets both in
394 temperature and relative humidity above 25°N latitude. Thus, caution is advised in using INSAT-
395 3D data over those locations. It is important to note that INSAT-3D shows good agreement with
396 the conventional in-situ radiosonde observations of both Gadanki and IMD locations over the
397 Indian region giving a sign of good reliability to use the former datasets for measuring the
398 temperature and relative humidity spatially and temporally. Very low difference in temperature
399 between INSAT-3D and radiosonde observations provides the scope of using the INSAT-3D
400 data into the numerical weather models for better forecasts. However, caution is again advised
401 while using the RH where most of the time a mean dry bias of 20-30% is noticed. Though
402 consistent positive bias of ~2-3 K is observed in the cold point tropopause temperatures, the
403 variability in tropopause obtained from INSAT-3D shows excellent match with the in-situ
404 radiosonde observations during 2014 and 2015. Thus, INSAT-3D data can also be used to study



405 the tropopause characteristics at sub-daily scales which are not possible with any existing
406 satellites and hence Stratosphere-Troposphere Exchange processes.

407

408 **Acknowledgements:** The INSAT-3D data used in the present study obtained from MOSDAC is
409 greatly acknowledged. We thank AIRS, MLS, ERA-Interim and NCEP teams for providing data
410 used in the present study through their ftp sites.



411 **References**

- 412 Aumann, H., Moustafa, T.C., Gautier, C., Mitchell, D.G., Kalnay, E., McMillin, L.,
413 Revercomb, H., Rosenkranz, P.W., Smith, W.L., Staelin, D., Strow, L., Susskind, J.:
414 AIRS/AMSU/HSB on the Aqua mission: Design, science objectives, data products and
415 processing system, *IEEE Trans. Geosci. Remote Sens.*, 41, 253 – 264, 2003.
- 416 Basha, G., and Venkat Ratnam, M.: Identification of atmospheric boundary layer height over a
417 tropical station using high resolution radiosonde refractivity profiles: Comparison with GPS
418 radio occultation measurements, *J. Geophys. Res.*, 114, D16101, doi:10.1029/2008JD011692,
419 2009.
- 420 Basha, G., Venkat Ratnam, M., Krishna Murthy, B.V.: Upper tropospheric water vapour
421 variability over tropical latitudes observed using radiosonde and satellite measurements,
422 *Article, J. Earth Sys. Sci.*, 122, 6, 1583-1591, 2013.
- 423 Durre, I., Vose, R., Wuertz, D.: Overview of the Integrated Global Radiosonde Archive, *J. Clim.*,
424 19, 53–68, 2006.
- 425 Hayden, C.M.: GOES-VAS simultaneous temperature-moisture retrieval algorithm, *J. Appl.*
426 *Meteor.*, 27, 705-733, 1988.
- 427 Kalnay, E., Kanamitsu, M., Kistler, R., Collins, W., Deaven, D., Gandin, L., Iredell, M., Saha, S.,
428 White, G., Woollen, J., Zhu, Y., Chelliah, M., Ebisuzaki, W., Higgins, W., Janowiak, J., Mo,
429 K.C., Ropelewski, C., Wang, J., Leetmaa, A., Reynolds, R., Roy Jenne., Dennis Joseph: The
430 NCEP/NCAR 40-year reanalysis project, *Bull. Am. Meteor. Soc.*, 7, 437–471, 1996 .
- 431 Kaplan, L. D.: Inference of atmospheric structure from remote radiation measurements, *Journal*
432 *of the Optical Society of America.*, 49, 1004, 1959.



- 433 Li, J., Huang, H.L.: Retrieval of atmospheric profiles from satellite sounder measurements by
434 use of the discrepancy principle, *Appl. Optics.*, Vol. 38, No. 6, 916-923, 1999.
- 435 Livesey, N.J., Snyder, W.V., Read, W.G., Wagner, P.A.: Retrieval algorithms for the EOS
436 Microwave Limb Sounder (MLS) instrument, *IEEE Trans. Geosci. Remote Sensing.*, 44, no. 5,
437 1144-1155, doi:10.1109/TGRS.2006.872327, 2006.
- 438 Ma, X.L., Schmit, T., Smith, W.: A non-linear physical retrieval algorithm – Its application to
439 the GOES-8/9 sounder, *J. Appl. Meteor.*, 38,501-503, 1999.
- 440 Mitra, A. K., Bhan, S. C., Sharma, A. K., Kaushik, N., Parihar, S., Mahandru, R., Kundu, P. K.:
441 INSAT-3D vertical profile retrievals at IMDPS, New Delhi: A preliminary evaluation,
442 *Mausam*, 66(4), 687-694, 2015.
- 443 Mehta, S.K., Venkat Ratnam, M., Krishna Murthy, B.V.: Variability of the tropical tropopause
444 over Indian monsoon region, *J. Geophys. Res.*, 115, D14120, doi:1029/2009JD012655, 2010.
- 445 Newell, R. E., Kidson, J.W., Vincent, D. G.: Annual and biennial modulations in the tropical
446 Hadley cell circulation, *Nature.*, 222, 76-78, 1969.
- 447 Reed, R. J., Vlcek, C. L.: The annual temperature variation in the lower stratosphere, *J. Atmos.*
448 *Sci.*, 26, 163-167, 1969.
- 449 Reid, G. C., Gage, K. S.: The tropical tropopause over western Pacific: wave driving,
450 convection, and the annual cycle, *J. Geophys. Res.*, 101:21233–21241, 1996.
- 451 Siedel, D. J., Ross, R. J., Angell, J.K., Reid, G. C.: Climatological characteristics of the tropical
452 tropopause as revealed by radiosondes, *J. Geophys. Res.*, 106:7857–7878, 2001.
- 453 Simmons, A. J., Hollingsworth, A.: Some aspects of the improvement in skill of numerical
454 prediction, *Q. J. R. Meteorol. Soc.*, 128, 647–677, 2002.
- 455 Simmons, A., Uppala, S., Dee, D.: Update on ERA-Interim, *ECMWF Newsl.*, 111, 5, 2007.



- 456 Susskind, J., Barnet, C. D., Blaisdell, J. M., Iredell, L., Keita, F., Kouvaris, L., Molnar, G.,
457 Chahine, M.: Accuracy of geophysical parameters derived from Atmospheric Infrared
458 Sounder/Advanced Microwave Sounding Unit as a function of fractional cloud cover, J.
459 Geophys. Res., 111(D9), D09s17, doi:10.1029/2005jd006272,2006.
- 460 Trenberth, K.E., Stepaniak, D.K.: Seamless poleward atmospheric energy transports and
461 implications for the Hadley circulation, J.Clim., 16, 3706-3722,2003a.
- 462 Trenberth, K.E., Stepaniak, D.K.: Covariability of components of poleward atmospheric energy
463 transports on seasonal and inter annual timescales, J.Clim., 16, 3691-3705,2003b.
- 464 Venkat Ratnam, M., Tsuda, T., Shiotani, M., Fujiwara, M.: New Characteristics of the Tropical
465 Tropopause Revealed by CHAMP/GPS Measurements, SOLA, Vol. 1, 185–188,
466 doi:10.2151/sola.2005–048,2005.
- 467 Venkat Ratnam, M., Pravalika, N., Ravindra Babu, S., Bahsa, G., Krishna Murthy, B.V.:
468 Assesment of GPS radiosonde descent data, Atmos. Meas.Tech.,7,1011-1025,2014.
- 469 Venkat Ratnam, M., Sunil Kumar, S.V., Parameswaran, K., Krishna Murthy., Ramkumar, G.,
470 Rajeev, K., Ghouse Basha., Ravindra Babu, S., Muhsin, M., Manoj Kumar Mishra., Hemanth
471 Kumar, A., AkhilRaj, S.T., Pramitha, M.:Tropical tropopause dynamics (TTD) campaigns
472 over Indian region: An overview, J. Atmos. Sol. Terr. Phys.,
473 <http://dx.doi.org/10.1016/j.jastp.2014.05.007>,2014.
- 474 Venkat Ratnam, M., Basha, G., Krishna Murthy, B.V., Jayaraman, A.: Relative humidity
475 distribution from SAPHIR experiment on board Megha-Tropiques satellite mission:
476 Comparison with global radiosonde and other satellite and reanalysis datasets, J. Geophys.
477 Res., 18, 1-9,doi:10.1002/jgrd.50699,2013



478 Waters, J.W., Froidevaux, L., Harwood, R.S., Jarnot, R.F., Pickett, H.M., Read, W.G., Siegel,
479 P.H., Cofield, R.E., Filipiak, M.J., Flower, D.A., Holden, D.R., Lau, G.K., Livesey, N.J.,
480 Manney, G.L., Pumphrey, H.C., Santee, M.L., Wu, D.L., Cuddy, D.T., Lay, R.R., Loo, M.S.,
481 Perun, V.S., Schwartz, M.J., Stek, P.C., Thurstans, R.P., Boyles, M.A., Chandra, S., Chavez,
482 M.C., Chen, G.S., Chudasama, B.V., Dodge, R., Fuller, R.A., Girard, M.A., Jiang, J.H.,
483 Jiang, Y., Knosp, B.W., LaBelle, R.C., Lam, J.C., Lee, K.A., Miller, D., Oswald, J.E., Patel,
484 N.C., Pukala, D.M., Quintero, O., Scaff, D.M., Snyder, W.V., Tope, M.C., Wagner, P.A.,
485 Walch, M.J.: The Earth Observing System Microwave Limb Sounder (EOS MLS) on the Aura
486 satellite, IEEE Trans. Geosci. Remote Sensing, 44, no. 5, doi:10.1109/TGRS.2006.873771,
487 2006.
488



489 **Figure captions:**

490 **Figure 1.** Spatial variation of (a) temperature and (b) relative humidity over Indian region at 850
491 hPa pressure level obtained from INSAT-3D satellite on 2 May 2015 (averaged over a day).
492 The filled circles (magenta) in both the panels show the locations of IMD radiosonde stations
493 selected within 0-40°N latitude and 60-100°E longitude (Indian region) for comparing INSAT-
494 3D observations. White patches show the non-availability of the data.

495 **Figure 2.** Spatial variation of temperature over Indian region at 500 hPa pressure level obtained
496 from (a) INSAT-3D, (b) MLS, (c) AIRS, (d) ERA-Interim and (e) NCEP on 2 May 2015
497 around 1330 IST. (f) – (j) same as (a) to (e) but for relative humidity. White patches show the
498 non-availability of the data.

499 **Figure 3:** Temporal variation of (a) temperature and (b) relative humidity obtained from
500 radiosonde launched over Gadanki during the TTD Campaign conducted from 27 Jan. 2014 to
501 30 Jan. 2014. White patches show the non-availability of the data. (c) and (d) same as (a) and
502 (b) but observed by INSAT-3D. The mean profiles of (e) temperature and (f) relative humidity
503 obtained from radiosonde (red) and INSAT-3D (blue). Horizontal lines indicate standard
504 deviations.

505 **Figure 4:** Correlation coefficients obtained in (a) temperature and (b) relative humidity at
506 different pressure levels between INSAT-3D and 12 UTC Gadanki radiosondes (red line) and
507 00 UTC IMD radiosondes (black line). Horizontal bars show the deviations in correlation
508 coefficients obtained from 34 stations. Note that correlation coefficient up to 300 hPa is only
509 obtained for relative humidity.

510 **Figure 5:** Mean difference (thick line) and standard deviation (dotted lines) observed in the
511 temperature between INSAT-3D and radiosonde launched at around 12UTC over Gadanki



512 during 2014 and 2015. The blue line in (a) represents the number of radiosondes reaching at
513 different altitudes with top-right axis.

514 **Figure 6:** Zonal mean latitudinal difference between the INSAT-3D temperature and (a) AIRS,
515 (b) MLS, (c) ERA-Interim and (d) NCEP temperatures observed during 2014 and 2015. The
516 contours whose differences are within 1K are omitted.

517 **Figure 7:** Zonal mean latitudinal difference between the INSAT-3D RH and (a) AIRS RH, (b)
518 MLS RH, (c) ERA-Interim RH, (d) NCEP RH and (e) SAPHIR RH observed during 2014 and
519 2015. White patches show the non-availability of the data. The dotted (thick) line contours
520 show the negative (positive) differences between INSAT-3D and respective data sets.

521 **Figure 8:** Time series of cold point tropopause temperatures (CPT) observed over Gadanki
522 during 2014 and 2015 by INSAT-3D (blue line) and radiosonde (red line) at 12 UTC. These
523 are the 5-point running average of CPT.

524

525

526 **Table caption:**

527 **Table 1:** The principal absorbing gases of the Infrared radiation in the atmosphere at different
528 channels in INSAT-3D with their central wavelengths and their purpose of retrieval.

529



530 **Table 1:** The principal absorbing gases of the Infrared radiation in the atmosphere at different
 531 channels in INSAT-3D with their central wavelengths and their purpose of retrieval.

532
 533

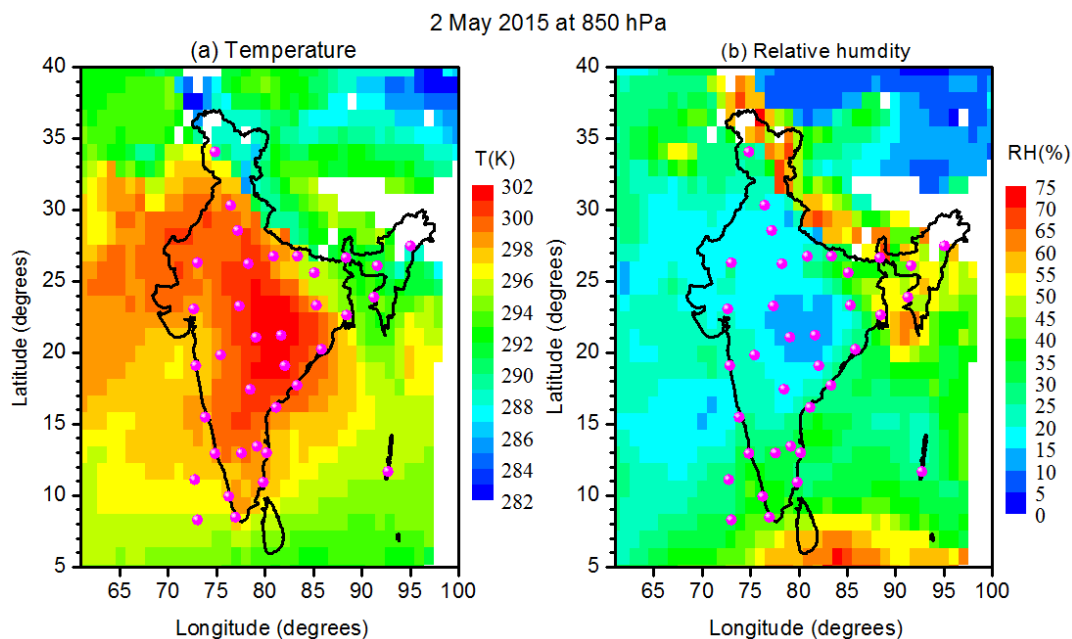
Detector	Ch. No.	Wavelength(μm)	Principal absorbing gas	Purpose
Long wave	1	14.67	CO ₂	Stratosphere temperature
	2	14.31	CO ₂	Tropopause temperature
	3	14.03	CO ₂	Upper-level temperature
	4	13.64	CO ₂	Mid-level temperature
	5	13.33	CO ₂	Low level temperature
	6	12.59	Water vapor	Total precipitable water
Mid wave	7	11.98	Water vapor	Surface temperature, moisture
	8	10.99	Window	Surface temperature
	9	9.69	Ozone	Total ozone
	10	7.43	Water vapor	Low level moisture
	11	7.04	Water vapor	Mid-level moisture
	12	6.52	Water vapor	Upper level moisture
Short wave	13	4.61	N ₂ O	Low level temperature
	14	4.54	N ₂ O	Mid-level temperature
	15	4.48	CO ₂	Upper level temperature
	16	4.15	CO ₂	Boundary level temperature
	17	4.01	Window	Surface temperature
	18	3.79	Window	Surface temperature, moisture

534
 535



536 **Figures**

537



538

539 **Figure 1.** Spatial variation of (a) temperature and (b) relative humidity over Indian region at 850

540 hPa pressure level obtained from INSAT-3D satellite on 2 May 2015 (averaged over a day).

541 The filled circles (magenta) in both the panels show the locations of IMD radiosonde stations

542 selected within 0-40°N latitude and 60-100°E longitude (Indian region) for comparing INSAT-

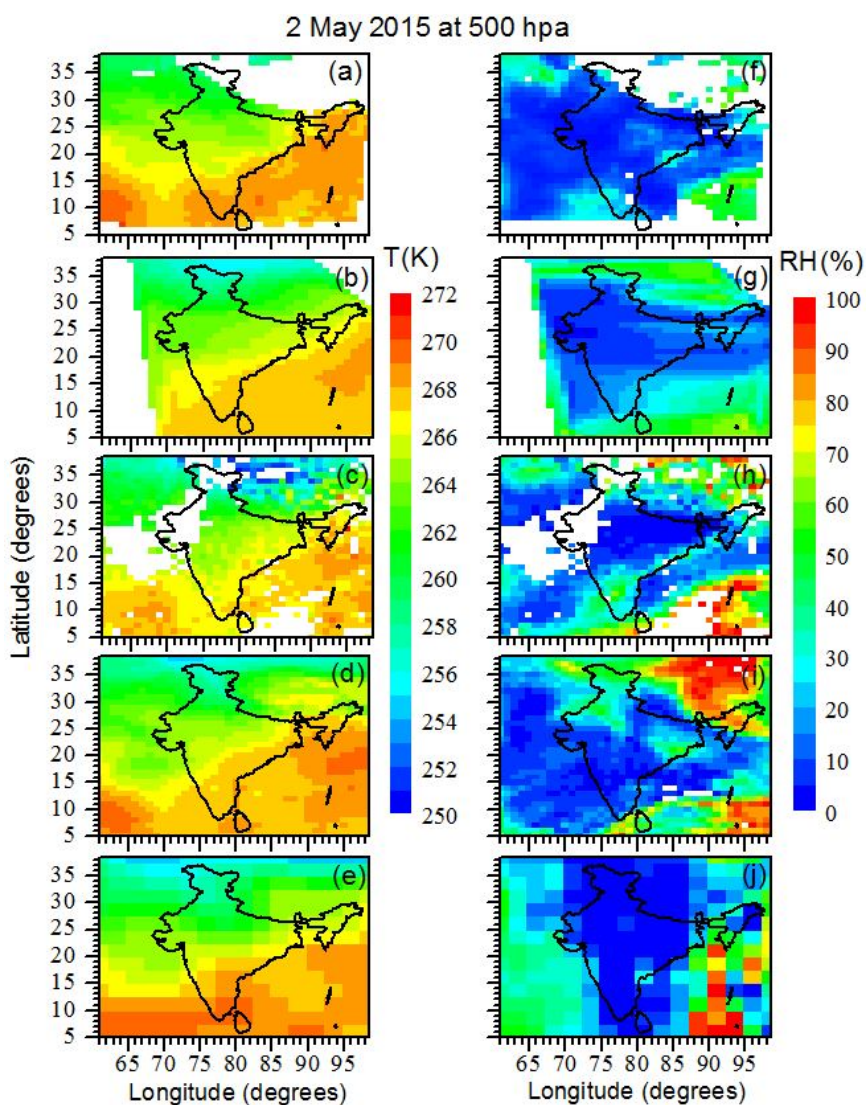
543 3D observations. White patches show the non-availability of the data.

544

545



546



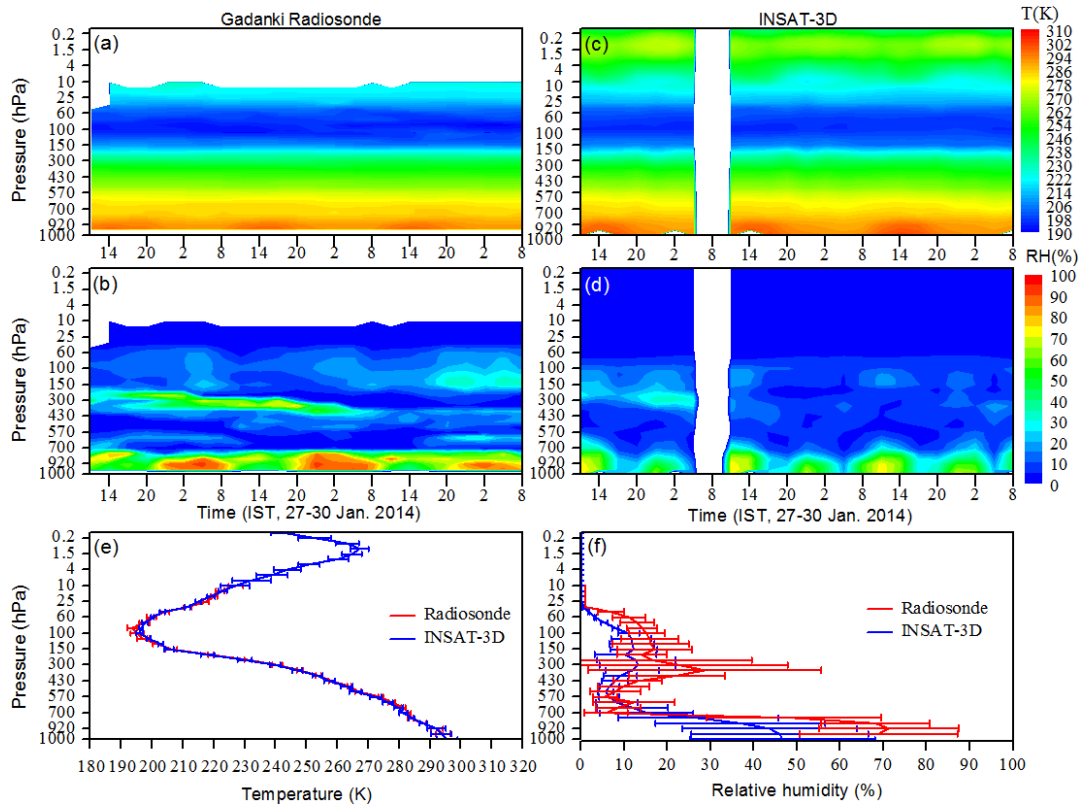
547

548 **Figure 2.** Spatial variation of temperature over Indian region at 500 hPa pressure level obtained
549 from (a) INSAT-3D, (b) MLS, (c) AIRS, (d) ERA-Interim and (e) NCEP on 2 May 2015
550 around 1330 IST. (f) – (j) same as (a) to (e) but for relative humidity. White patches show the
551 non-availability of the data.

552



553



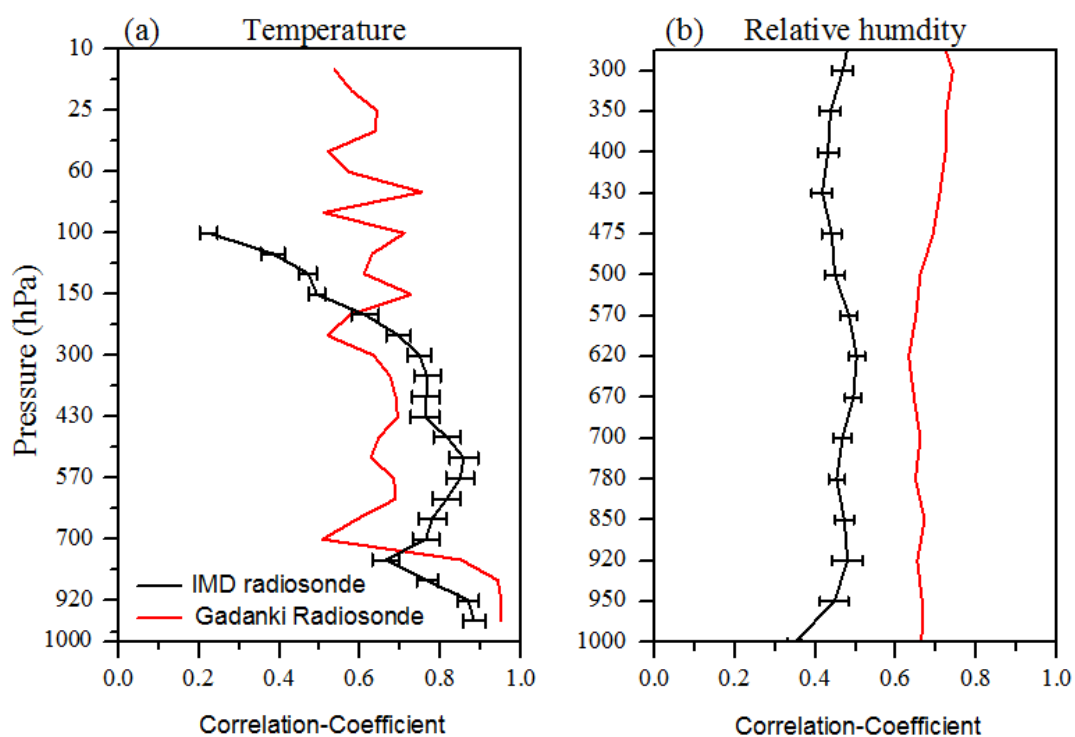
554

555 **Figure 3:** Temporal variation of (a) temperature and (b) relative humidity obtained from
 556 radiosonde launched over Gadanki during the TTD Campaign conducted from 27 Jan. 2014 to
 557 30 Jan. 2014. White patches show the non-availability of the data. (c) and (d) same as (a) and
 558 (b) but observed by INSAT-3D. The mean profiles of (e) temperature and (f) relative humidity
 559 obtained from radiosonde (red) and INSAT-3D (blue). Horizontal lines indicate standard
 560 deviations.

561



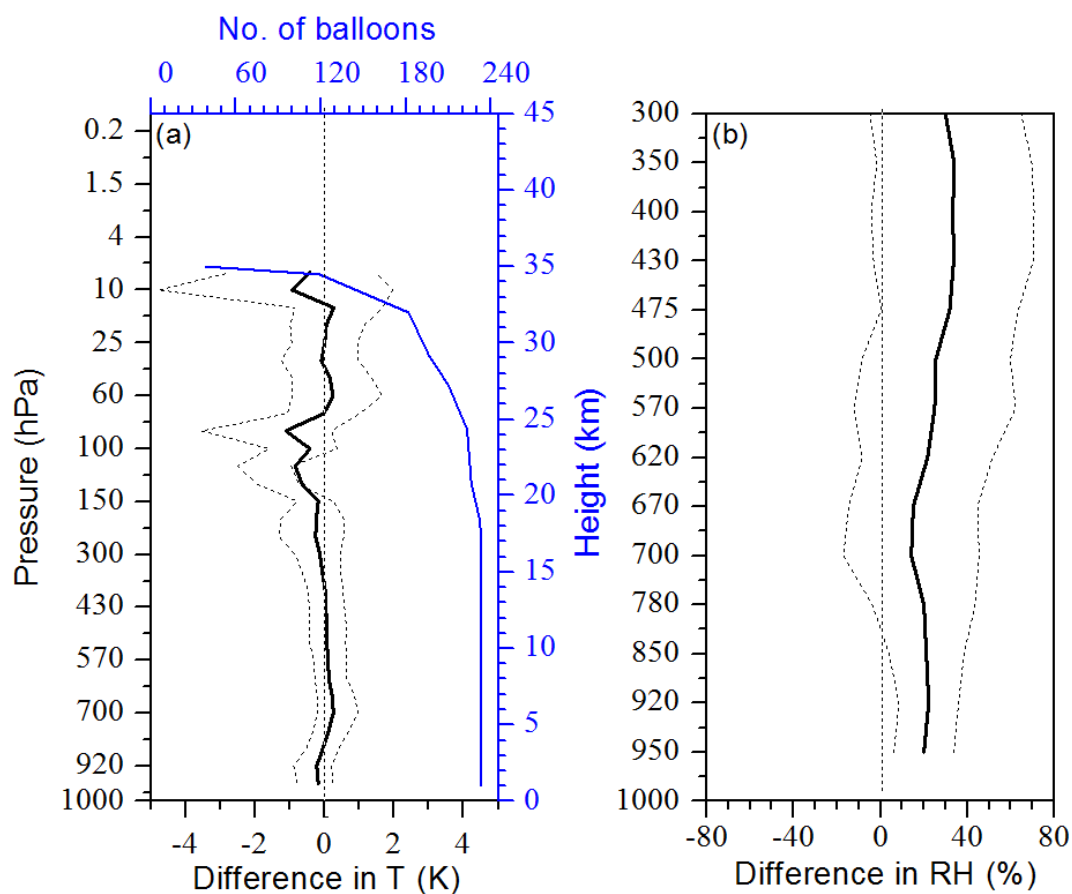
562



563

564 **Figure 4:** Correlation coefficients obtained in (a) temperature and (b) relative humidity at
565 different pressure levels between INSAT-3D and 12 UTC Gadanki radiosondes (red line) and
566 00 UTC IMD radiosondes (black line). Horizontal bars show the deviations in correlation
567 coefficients obtained from 34 stations. Note that correlation coefficient up to 300 hPa is only
568 obtained for relative humidity.

569



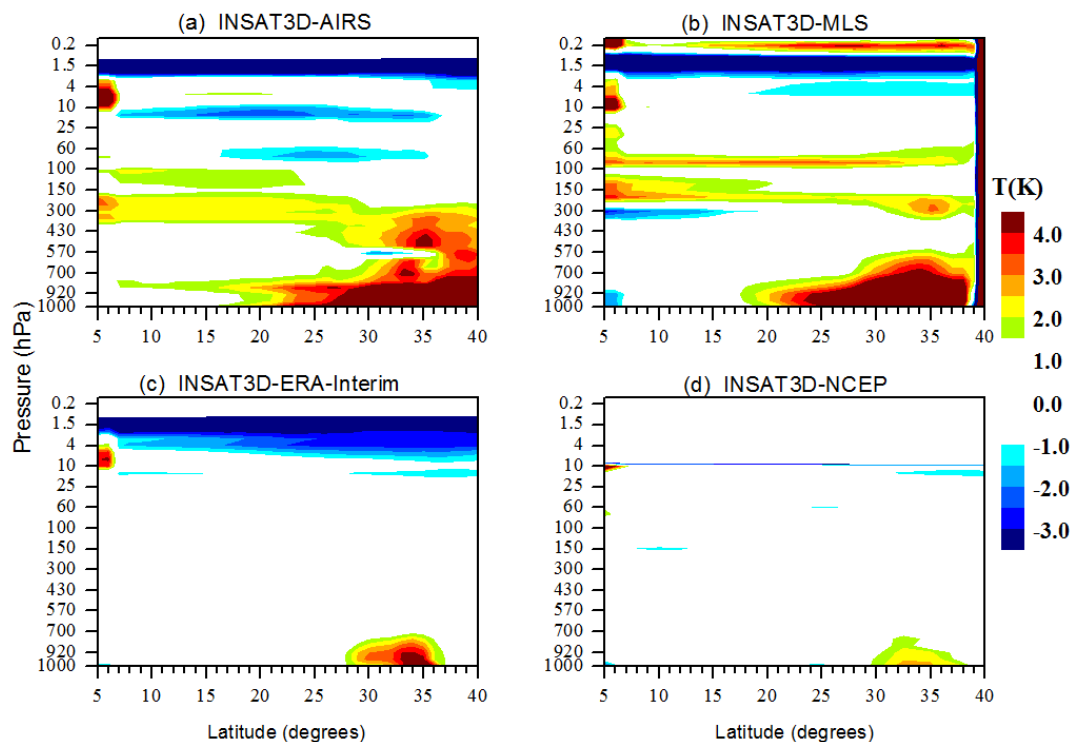
570

571 **Figure 5:** Mean difference (thick line) and standard deviation (dotted lines) observed in the
572 temperature between INSAT-3D and radiosonde launched at around 12UTC over Gadanki
573 during 2014 and 2015. The blue line in (a) represents the number of radiosondes reaching at
574 different altitudes with top-right axis.

575



576



577

578 **Figure 6:** Zonal mean latitudinal difference between the INSAT-3D temperature and (a) AIRS,
579 (b) MLS, (c) ERA-Interim and (d) NCEP temperatures observed during 2014 and 2015. The
580 contours whose differences are within 1K are omitted.

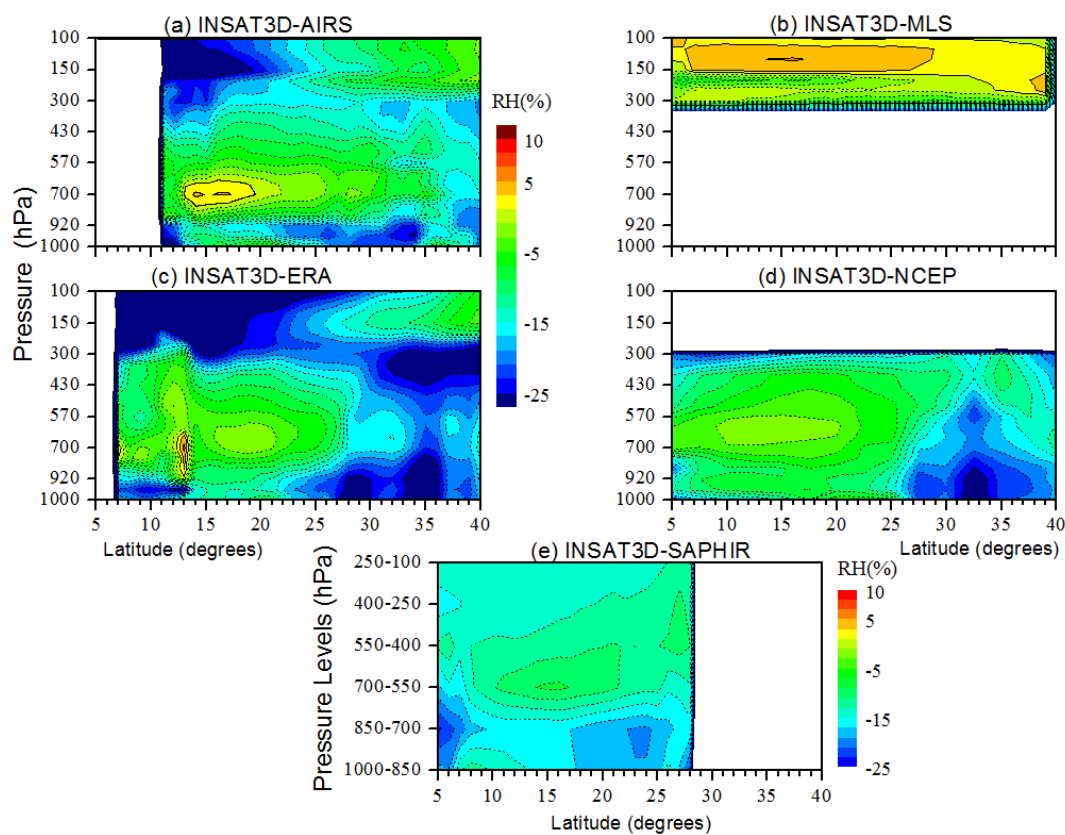
581

582

583



584



585

586 **Figure 7:** Zonal mean latitudinal difference between the INSAT-3D RH and (a) AIRS RH, (b)

587 MLS RH, (c) ERA-Interim RH, (d) NCEP RH and (e) SAPHIR RH observed during 2014 and

588 2015. White patches show the non-availability of the data. The dotted (thick) line contours

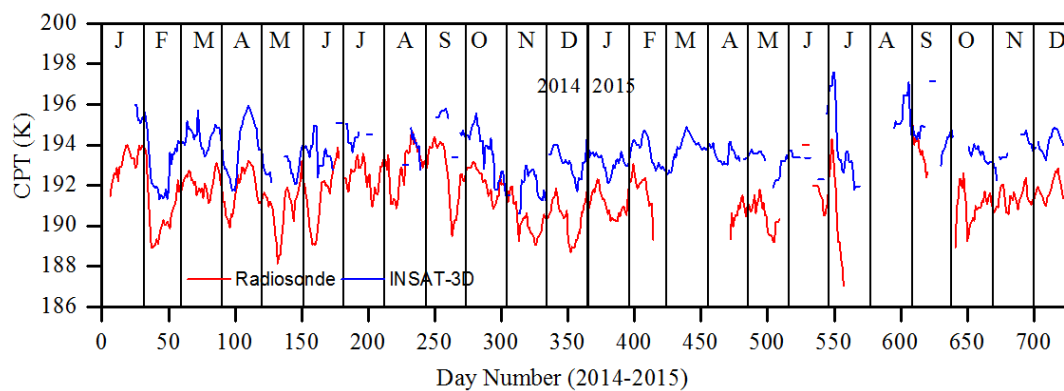
589 show the negative (positive) differences between INSAT-3D and respective data sets.

590

591



592



593

594 **Figure 8:** Time series of cold point tropopause temperatures (CPT) observed over Gadanki
595 during 2014 and 2015 by INSAT-3D (blue line) and radiosonde (red line) at 12 UTC. These
596 are the 5-point running average of CPT.

597